Article

Parameter Estimation of a Thermoelectric Generator by Using Salps Search Algorithm

Daniel Sanin-Villa [1] **, Oscar Danilo Montoya** [2] **, Walter Gil-González** [3] **, Luis Fernando Grisales-Noreña** [4,*] **and Alberto-Jesus Perea-Moreno** [5,*]

[1] Departamento de Mecatrónica y Electromecánica, Instituto Tecnológico Metropolitano, Medellín 050036, Colombia; danielsanin@itm.edu.co
[2] Grupo de Compatibilidad e Interferencia Electromagnética (GCEM), Facultad de Ingeniería, Universidad Distrital Francisco José de Caldas, Bogotá 110231, Colombia; odmontoyag@udistrital.edu.co
[3] Department of Electrical Engineering, Faculty of Engineering, Universidad Tecnológica de Pereira, Pereira 660003, Colombia; wjgil@utp.edu.co
[4] Department of Electrical Engineering, Faculty of Engineering, Universidad de Talca, Curicó 3340000, Chile
[5] Departamento de Física Aplicada, Radiología y Medicina Física, Universidad de Córdoba, Campus de Rabanales, 14071 Córdoba, Spain
* Correspondence: luis.grisales@utalca.cl (L.F.G.-N.); aperea@uco.es (A.-J.P.-M.)

Abstract: Thermoelectric generators (TEGs) have the potential to convert waste heat into electrical energy, making them attractive for energy harvesting applications. However, accurately estimating TEG parameters from industrial systems is a complex problem due to the mathematical complex non-linearities and numerous variables involved in the TEG modeling. This paper addresses this research gap by presenting a comparative evaluation of three optimization methods, Particle Swarm Optimization (PSO), Salps Search Algorithm (SSA), and Vortex Search Algorithm (VSA), for TEG parameter estimation. The proposed integrated approach is significant as it overcomes the limitations of existing methods and provides a more accurate and rapid estimation of TEG parameters. The performance of each optimization method is evaluated in terms of root mean square error (RMSE), standard deviation, and processing time. The results indicate that all three methods perform similarly, with average RMSE errors ranging from 0.0019 W to 0.0021 W, and minimum RMSE errors ranging from 0.0017 W to 0.0018 W. However, PSO has a higher standard deviation of the RMSE errors compared to the other two methods. In addition, we present the optimized parameters achieved through the proposed optimization methods, which serve as a reference for future research and enable the comparison of various optimization strategies. The disparities observed in the optimized outcomes underscore the intricacy of the issue and underscore the importance of the integrated approach suggested for precise TEG parameter estimation.

Keywords: thermoelectric generators; master–slave strategy; root mean square error standard deviation; standard deviation analysis

1. Introduction

Mixed integer non-linear programming problems (MINLP) represent a general class of optimization problems encompassing a wide range of complex, real-world applications in engineering, science, and economics [1,2]. They pose a significant computational challenge owing to the presence of both integer and continuous decision variables, non-linear objective functions and constraints, and active inequality and equality constraints. Consequently, there is no universal algorithm for solving all instances of MINLPs, and specialized techniques and algorithms are required to tackle this class of problems [3]. One of the primary difficulties in solving MINLPs is the presence of non-convexities in the objective function and constraints, which can result in multiple local optima and make the global optimization problem more challenging [4]. Moreover, active constraints complicate the problem even

further, as the optimizer must search through continuous and discrete solution spaces while satisfying all the constraints [5].

Despite the inherent challenges, MINLPs have significant real-world implications and find applications in diverse areas such as heat and mass exchange networks [6], batch plant design [7], scheduling, and interplanetary spacecraft trajectory design [8]. Solving these problems can result in substantial cost savings, improved efficiency, and decision-making processes in numerous industries.

A general form of a Mixed Integer Non-Linear Programming (MINLP) problem can be expressed mathematically as follows: [9]:

$$\min_{x,y} f(x,y) \quad \text{subject to: } x \in \mathbb{R}^n \quad y \in \mathbb{Z}^m \quad g_i(x,y) \le 0, \; i = 1, 2, \ldots, p \quad h_j(x,y) = 0, \; j = 1, 2, \ldots, q$$

where x represents the continuous decision variables, y denotes the integer decision variables, $f(x,y)$ is the non-linear objective function, $g_i(x,y) \le 0$ represents the inequality constraints, and $h_j(x,y) = 0$ is the equality constraints. The optimization problem aims to minimize the non-linear objective function subject to the given constraints.

The constraints ensure that the decision variables satisfy the problem requirements and limitations. The integer decision variables y are restricted to integer values, while the continuous decision variables x can take any real value. The objective function and constraints are generally non-linear, making the problem challenging to solve, and there may be multiple local minima or maxima. The optimal solution is achieved when the objective function is minimized subject to all constraints being satisfied.

Mixed integer non-linear programming problems pose a significant computational challenge, but they have crucial real-world and engineering applications. The development of specialized algorithms and techniques for solving these problems is a crucial area of research that has the potential to improve industrial processes significantly. The solution to MINLPs problems has been the subject of intensive research over the years, leading to the development of various optimization solvers. These solvers can be broadly classified into deterministic [10] and stochastic methods [11–13]. Deterministic methods aim to find the optimal solution to the MINLP problem by iteratively exploring the feasible region of the problem. These methods usually involve branch-and-bound algorithms that divide the problem into smaller sub-problems and explore their feasible regions exhaustively. Using linear relaxations to bound the integer variables' feasible regions often guides the branch-and-bound search, resulting in an efficient algorithm. Other deterministic methods include outer approximation, mixed-integer linear programming, and convex relaxations. Deterministic methods have been successful in solving small-to-medium-sized MINLP problems where the computational time required is feasible. However, for large-scale problems, these methods may become computationally expensive and not practical. On the other hand, stochastic methods are based on probabilistic search techniques and randomly explore the solution space. These methods aim to find good-quality solutions faster than deterministic methods, with a trade-off between solution quality and computational cost. Stochastic methods include genetic algorithms [14], simulated annealing [15], tabu search [16], particle swarm optimization [17,18], and Salps search algortithm [19,20]. Other works have proposed a novel framework to improve intrusion detection system (IDS) performance based on deep learning and metaheuristic optimization algorithms. They also introduce a new feature selection mechanism based on a recently developed metaheuristic method called Reptile Search Algorithm (RSA) [21] and heuristic method to build a recommender engine in IoT environment exploiting swarm intelligence techniques [22]. These methods are particularly useful when the problem's objective function and constraints are complex and non-linear and the search space is high-dimensional. Although stochastic methods can handle large-scale problems efficiently, they may converge to sub-optimal solutions, and the quality of the solution heavily depends on the selection of the algorithm's parameters.

Thermoelectric generators (TEGs) convert heat energy directly into electrical energy using the Seebeck effect [23]. The performance of TEGs depends on the materials used to construct them, which determine their thermoelectric properties. The parameters that

govern the thermoelectric behavior of a TEG can be modeled using mathematical expressions [24], and the values of these parameters can be estimated using empirical data and metaheuristic algorithms [25]. However, one of the main challenges in designing efficient TEGs is accurately estimating the relevant parameters, such as the Seebeck coefficient, electrical conductivity, and thermal conductivity, which determine the device's overall energy conversion efficiency. In particular, parameter estimation of TEGs is a complex problem from an energy point of view, since it requires balancing competing requirements, such as maximizing the electrical output while minimizing the heat loss. Furthermore, the performance of TEGs is highly dependent on the materials used, and accurately characterizing their properties is a difficult task that requires advanced measurement techniques and computational models to characterize and control the TEG devices in real applications. Therefore, developing accurate and reliable methods for parameter estimation of TEGs remains a significant challenge for researchers in the field, and represents a critical step toward realizing the full potential to extract the power from this promising technology. Empirical data refer to experimental TEG performance measurements under different operating conditions; these data can be used to calibrate the model parameters and validate the model's accuracy. Metaheuristic algorithms, on the other hand, are optimization algorithms that can search for optimal values of the model parameters by exploring the parameter space randomly. One approach to model TEG parameters is to use a regression model based on empirical data. The regression model forms a mathematical expression that relates the TEG's output power generation and current to the input temperature difference at the cold and hot sides of the TEG. Metaheuristic algorithms are reliable solutions to optimize those problems and find the TEG parameters directly. The parameter space can include thermal material properties, geometric dimensions, and electrical properties. Metaheuristic algorithms can explore the parameter space efficiently and provide near-optimal solutions. It is crucial to accurately estimate the power output delivered by TEG modules for practical applications such as power generation in waste heat recovery [26], medical applications [27], or nuclear heat engines for space explorations [28]. To achieve this, it is important to understand the temperature conditions at the boundaries of the TEG modules [24]. These temperature conditions do not constantly change but vary slowly over time. Therefore, studying temperature conditions with known parameters becomes important for industrial applications and advancements in TEG technology. One approach to modeling the performance of TEG modules is to develop mathematical models that consider the temperature conditions at the boundaries of the modules. These models can be calibrated using empirical data and validated through experimentation. The power output delivered at constant temperatures can be estimated by accurately modeling the temperature conditions and the thermoelectric behavior of the TEG modules. This information is critical for designing TEG systems arrays that can operate efficiently and deliver the desired power output under varying temperatures and mismatched thermal conditions [29].

Despite the significant progress made in analyzing thermoelectric generator modules, there remains a critical need to develop a methodology based on optimization algorithms that can accurately characterize these modules under varying temperature conditions. The literature lacks a comprehensive methodology that considers all thermoelectric effects analyzed in complex and differential models, resulting in a significant gap in both academic and industrial applications that require fast and accurate responses. To address this gap, advanced optimization techniques need to be developed that can effectively capture the complex interplay between temperature conditions and thermoelectric properties' behavior while accounting for the stochastic nature of experimental results. This research focuses on characterizing thermoelectric generator modules by utilizing mathematical and programming techniques based on experimental data. The ultimate goal is to improve the model parameter to maximize the efficiency of energy harvesting from waste heat and other heat sources. Inadequate characterization of material properties and TEG parameters can result in inaccurate modeling of heat transfer and thermal gradients. This, in turn, can lead to inaccuracies in estimating performance metrics and power control. Therefore,

achieving an accurate characterization of TEG modules is crucial for optimizing energy conversion and harvesting from waste heat or any other heat sources. This work has made several significant contributions to the field of thermoelectric generation (TEG), both in academia and industry. In terms of academic contributions, specialized algorithms and techniques have been developed for solving Mixed Integer Non-Linear Programming (MINLP) problems applied to TEG systems. Additionally, mathematical models have been developed that capture the thermal and electrical material properties of TEGs. Finally, the use of metaheuristic algorithms has been investigated as a means of estimating model parameters, which can improve TEG performance and energy efficiency. In terms of industrial contributions, MINLP problems have been applied in diverse areas such as waste heat recovery energies. Furthermore, specialized algorithms and techniques for solving MINLP problems have been developed and implemented in real-world industries, leading to improved decision-making processes. Finally, the use of metaheuristic algorithms for estimating model parameters in TEGs has led to the development of more efficient and cost-effective industrial applications. Overall, this work has made significant contributions to the development and optimization of TEG systems for both academic and industrial purposes. The paper is structured into six sections. Section 1 provides an introduction to the study of the trade-off comparison between optimization algorithms to solve the MINLP problem in TEG applications. In Section 2, the Master–Slave methodology is presented in detail, which is developed to solve the MINLP problem in TEG applications, focusing on the mathematical modeling of the algorithms and the TEG module. Section 3 presents the experimental data used to test the proposed methodology. The comparison methods and criteria used to compare the performance of the different optimization algorithms are explained in Section 4. Section 5 presents the results of the parameter estimation obtained from the comparison of the optimization algorithms. Finally, Section 6 presents the conclusions drawn from this study, and the findings of this research can provide valuable insights for optimizing TEG modules in practical applications.

2. Master–Slave Strategy

The material property characterization and parameter estimation of a thermoelectric generator in this paper is carried out by using a master–slave strategy that using in the Salps Search Algorithm (SSA) in the master stage for solving the problem of parameter estimation of a TEG. In this stage, the SSA proposes in each iteration multiple configurations of parameters for the TEG analyzed, based on the information stored in the swarm of Salps. Each one of the solutions proposed for this is evaluated by the slave stage. The slave stage uses a mathematical formulation that evaluates the material property characterization by using the parameters proposed by the master stage, with the aim to obtain energy production in the TEG. This value is compared with real power measured in the TEG by obtaining the RMSE used by the SSA as the objective function. The SSA was chosen for this study due to its proven effectiveness in optimizing the parameter estimation of electrical devices, as demonstrated in previous research [30–32]. This optimization method is a bio-inspired algorithm that is based on the collective behavior of salps, gelatinous marine organisms that move in swarms to locate the best sources of food.

The mathematical model used in this study is derived from a phenomenological analysis of a TEG leg. This approach involves a detailed examination of the physical and chemical processes that occur within the leg and the development of mathematical equations that accurately represent these processes. By using a phenomenological model, it is possible to gain a deeper understanding of the behavior of the TEG leg and to develop optimization algorithms that are tailored to the specific characteristics of this device. The master–slave strategy here proposed is illustrated in Figure 1.
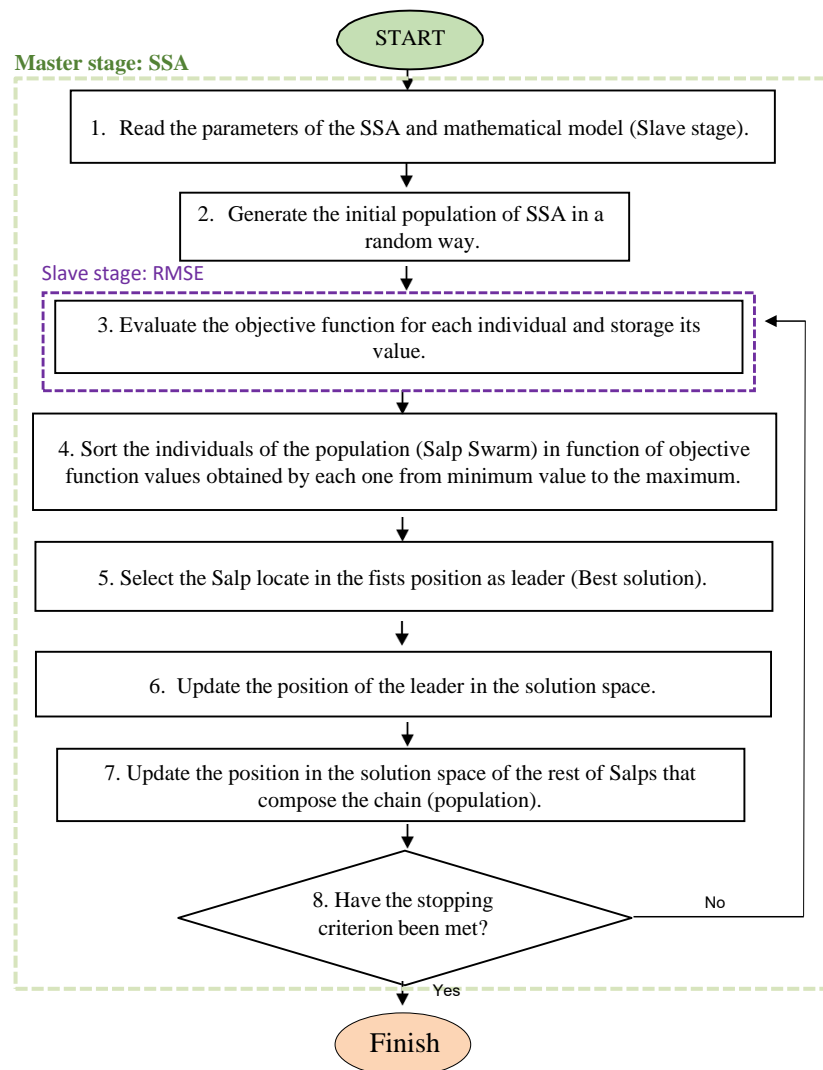
Figure 1. Master–slave methodology proposed SSA/RMSE.

In the master stage, SSA was used for solving the main problem: parameter estimation of a thermoelectric generator. This optimization method utilizes a population-based strategy inspired by nature, specifically the behavior of a family of marine organisms known as salps. These gelatinous barrel-shaped creatures extract plankton by filtering water as it passes through their bodies. Salps work in a chain-like formation, known as a swarm, with the goal of locating the optimal food source within the solution space. A designated leader guides the exploration of the salp chain, with each member updating its position based on the closest neighbor to the leader. The search and acquisition of food are mathematically modeled to represent the behavior of salps. This bio-inspired algorithm employs a population-based approach, where the goal is to obtain the best possible food source by tracking the leader. The swarm works together in a coordinated effort, with each member following the position of the closest neighbor to the leader. The algorithm is designed to mimic the complex behavior of these marine organisms, and its effectiveness in optimization has been demonstrated in various applications [33].

In the first step, the SSA generates the initial population in a random way, by generating the n individual that composes the solution. For carrying out this labor, Equation (1) is used. In this equation, *rand* is a random value between 0 and 1, while *ul* and *ll* correspond to the upper and lower limits of each variable used, i.e., all polynomial coefficients of material properties and geometrical parameters, which are presented in Figure 1. In this

figure, it is possible to appreciate the codification of size 1×11 used for representing the problem here analyzed.

$$Salps_{(i,j)} = ((ul - ll) \cdot rand) + lb \tag{1}$$

Table 1 reports left to right the coefficients of thermal conductivity (k_1, k_2, and k_3), the coefficients of the Seebeck material property (S_0, S_1, and S_2), and the coefficients related to electric resistivity (ρ_0, ρ_1, and ρ_2). Finally, we present the limits related to the equivalent number of legs of the TEG module (n_{legs}) and the effective cross-sectional area of a single TE leg (A_{cs}). A detailed explanation of those parameters on the TEG energy model is presented in the slave stage of this section.

Table 1. Thermoelectric generator's parameter limits.

Parameter	k_1	k_2	k_3	ρ_1	ρ_2	ρ_3	S_0	S_1	S_2	n_{legs}	A_{cs}
Upper limit	5.63	-3.50×10^{-2}	3.72×10^{-5}	8.38×10^{-7}	8.38×10^{-7}	-8.91×10^{-10}	4.60×10^{-7}	1.47×10^{-8}	5.65×10^{-11}	0	0.5×10^{-6}
Lower limit	6.98	-3.60×10^{-2}	4.54×10^{-5}	2.44×10^{-5}	1.02×10^{-6}	-1.09×10^{-9}	-5.62×10^{-7}	1.80×10^{-8}	6.91×10^{-11}	200	8×10^{-6}

Using Equation (1), we obtain the population of Salps illustrated in P_{Salps}, where S_n is the $n - esima$ salp in the swarm and $S_{(n,d)}$ is the parameter d of the salp n. The maximum value of d is equal to the number of parameters analyzed; in this particular case, it is eleven. It is important to highlight that each one of the salps contained in P_{Salps} is a solution to the problem here analyzed.

$$P_{Salps} = \begin{bmatrix} S_1 \\ S_2 \\ \vdots \\ \vdots \\ S_n \end{bmatrix} = \begin{bmatrix} S_{(1,1)} & S_{(1,2)} & \cdots & \cdots & S_{(1,d)} \\ S_{(2,1)} & S_{(2,2)} & \cdots & \cdots & S_{(2,d)} \\ \vdots & \vdots & \vdots & \vdots & \vdots \\ \vdots & \vdots & \vdots & \vdots & \vdots \\ S_{(n,1)} & S_{(n,2)} & \cdots & \cdots & S_{(n,d)} \end{bmatrix} \tag{2}$$

To generate the initial population, we evaluate the objective function (RMSE) associated with each Salp by using the slave stage. The RMSE value obtained by the swarm is stored in $RMSE_{Salps}$, by using Equation (3).

$$RMSE_{Salps} = \begin{bmatrix} RMSE\left(\left[S_{(1,1)}, S_{(1,2)}, \cdots, S_{(1,d)}\right]\right) \\ RMSE\left(\left[S_{(2,1)}, S_{(2,2)}, \cdots, S_{(2,d)}\right]\right) \\ \vdots \\ RMSE\left(\left[S_{(n,1)}, S_{(n,2)}, \cdots, S_{(n,d)}\right]\right) \end{bmatrix} \tag{3}$$

Then, the P_{Salps} and $RMSE_{Salps}$ are sorted from the lowest to the highest value obtained from the objective function, by selecting the Salp in the first position as the leader of the swarm (L^t_{Salps}), where t is the current iteration:

$$L^t_{Salps} = [S_{(1,1)}, S_{(1,2)}, \cdots, S_{(1,d)}] \tag{4}$$

The movement of the salps is led by the L_{Salps}, while the rest of Salps follow the leader in each iteration. For the movement of the next iteration t, L^{t+1}_{Salps}, we use Equation (5).

$$L^{t+1}_{Salps} = \begin{cases} L^t_{Salps} + C_1 * ((ub - lb) * C_2 + lb) & C_3 \leq 0.5 \\ L^t_{Salps} - C_1 * ((ub - lb) * C_2 + lb) & C_3 > 0.5 \end{cases} \tag{5}$$

The last equation allows the leader to follow two directions in the solution space based on a random value between 1 and 0 (C_3). By using the current values of the leader, two

components C_1 and C_2 add or rest a portion of each variable in a random way to the leader with the aim to move this in the region not explored in the solution space. C_1 is calculated using Equation (6), where t and t_{max} are the current iterations and the maximum number of iterations considered within the iterative process. C_2 is a random value between 0 and 1. Furthermore, this equation considers the minimum and maximum limits of variables that compose the problem.

$$C_1 = 2 * e^{-\left(\frac{4*t}{t_{max}}\right)^2} \tag{6}$$

The parameter C_1 controls the exploration velocity and step of the SSA, while C_1 and C_2 guarantee an adequate exploration of the solution space, avoiding the SSA and staying trapped in the local optimal.

$$S_i^{t+1} = \frac{1}{2}\left(S_{i-1}^{t+1} - S_i^t\right) \tag{7}$$

After identifying the new position of the leader in the iteration $t + 1$, we update the position of the rest of the salps that compose the chain or population by using Equation (7), by starting with the update of the position of the Salp located in the second position of the chain (swarm) until the last Salp, with the leader being the first individual of the chain. This equation takes advantage of the sorting made to the Salps in the function of the objective function. The position of the salp S_{i-1} is updated employing its information in the last iteration (t) and the information of the S_i obtained for current iteration $t + 1$.

Subsequently, it calculates the objective function for all Salps that compose the population, updating $RMSE_{Salps}$; the P_salps and $RMSE_{Salps}$ are sorted in relation to the minimum RMSE, selecting Salp in the first position as the new leader. The movement process described before is repeated by the SSA until it achieves the stopping criterion.

As a stopping criterion, the SSA employs a maximum number of iterations (t_max). So, the parameters that control the exploration of SSA are related to the size of the population and the t_max. In this paper, the Particle Swarm Optimization algorithm was used for tuning this parameter, finding a population size of 50 individuals and a maximum number of iterations equal to 1000.

2.1. Slave Stage

The RMSE is a widely used fitness function in optimization problems that aims to minimize the difference between observed and predicted values. In these problems, the RMSE serves as a measure of the model's accuracy in predicting the values of a dependent variable. The objective of the optimization problem is to determine the values of the independent variables that minimize the RMSE, which in turn maximizes the model's accuracy. When using the RMSE as the fitness function in an optimization problem, the objective is to find the input parameters that produce the lowest RMSE value. The optimization algorithm iteratively changes the input parameters and calculates the corresponding RMSE value until it finds the set of parameters that minimizes the RMSE. This process is known as parameter tuning and is commonly used in machine learning and data science to improve the accuracy of models. The RMSE is particularly useful in optimization problems where the objective is to fit a curve to a set of experimental data. The RMSE can be used to determine how well the curve fits the data and to select the best model. The model that produces the lowest RMSE value is considered the best fit for the data. A lower RMSE value indicates a stronger alignment between the model and the experimental data, signifying a higher level of accuracy. The optimization algorithm utilizes the RMSE as a fitness function to minimize the disparity between predicted and actual values, thereby identifying optimal parameters that minimize this disparity. The formal definition of the RMSE is expressed in Equation (8).

$$RMSE = \sqrt{\sum_{i=1}^{n} \frac{\left(\hat{W}_i - W_i\right)^2}{n}} \tag{8}$$

In order to calculate the estimated power values $\hat{W}_i$ corresponding to a specific current I, it is essential to develop a mathematical model that incorporates both the physical

parameters of the TEG module and the properties of the thermoelectric material. These properties vary with temperature, so temperature functions must be included in the model. In addition, the Thomson effect, which describes the coupling between temperature gradients and electric fields, must also be considered. The physical parameters of the TEG module that must be considered include the equivalent number of legs (n_{legs}), the effective cross-sectional area (A_{cs}), and the TE properties of a single TE element. The number of legs in a TEG module depends on the application; each leg consists of a p-type or an n-type thermoelectric material joined electrically in series and thermally in parallel. The effective cross-sectional area of a single TE leg measures the area available for heat transfer and is critical for determining the thermal performance of the TEG module.

In order to assess the accuracy of the mathematical model and validate its performance, it is crucial to compare the predicted power values with the corresponding experimental values W_i. The model's goodness of fit can be evaluated by utilizing the root mean square error (RMSE), which quantifies the discrepancy between the predicted and observed values. A smaller RMSE value indicates a stronger alignment between the model and the experimental data, thereby indicating a higher level of accuracy. In [24], a comprehensive model is presented to describe the thermoelectric behavior of a single TE leg. Equation (9) enables the calculation of the heat flux at both ends of an individual TEG leg. Simultaneously, the model predicts the total power output by multiplying the area-specific power output of a single leg by the quantity of equivalent legs within the TEG module, as illustrated in Equation (10).

$$q(x) = -k(T)\frac{dT}{dx} + jS(T)T(x) \tag{9}$$

$$W = n_{legs}A_{cs}(q_h - q_c) \tag{10}$$

The one-dimensional form of the energy model is represented by Equation (11), where j denotes the current density, calculated as $j = I/A_{cs}$, and $k(T)$, $S(T)$, $\rho(T)$, and T correspond to the thermal conductivity, Seebeck coefficient, electric resistivity, and temperature, respectively, at each point x along the leg length.

$$\frac{d}{dx}\left[k(T)\frac{dT}{dx}\right] - jT\frac{dS(T)}{dT}\frac{dT}{dx} + j^2\rho(T) = 0 \tag{11}$$

The functions $k(T)$, $S(T)$, and $\rho(T)$ can be expressed as second-degree polynomial functions of temperature, where the properties coefficients (S_0, S_1, S_2, ρ_0, ρ_1, ρ_2, k_1, k_2, k_3) are to be determined and were introduced before in Table 1. Specifically, Equation (12) represents the polynomial expression for $S(T)$, $\rho(T)$, and $k(T)$.

$$\begin{bmatrix} S(T) \\ \rho(T) \\ k(T) \end{bmatrix} = \begin{bmatrix} S_0 & S_1 & S_2 \\ \rho_0 & \rho_1 & \rho_2 \\ k_1 & k_2 & k_3 \end{bmatrix} \begin{bmatrix} 1 \\ T \\ T^2 \end{bmatrix} \tag{12}$$

To solve Equation (11) concerning TEGs and establish appropriate boundary conditions, a reliable numerical method needs to be utilized. In this particular scenario, a series of Dirichlet boundary conditions is defined in Equation (13), where T_c and T_h represent the temperatures at the cold and hot sides, respectively.

$$T|_{x=0} = T_c, \quad T|_{x=L} = T_h \tag{13}$$

Since the surface temperatures at the cold ($x = 0$) and hot sides ($x = L$) of a TEG module can be readily measured, it is reasonable to assume a linear temperature distribution for the second and third terms in Equation (11). This assumption is justified by Wee [34], who points out that the thermal conductivity of most thermoelectric materials is several orders of magnitude greater than the Thomson coefficient and electric resistivity. In the approximate analytical model presented by Ju et al. [35], an explicit solution is provided for the temperature profile described in Equation (11) of a single TEG leg (Equation (14)). This

solution aligns with previous findings addressing the same problem and is derived based on the aforementioned assumption. Intermediate variables computed as $\epsilon, \theta, u_0, u_1, u_2, C_1,$ and C_2 follow Equations (15)–(21).

$$T(x) = \frac{1}{4k_3}\left[4(\theta/2)^{1/3} - (2/\theta)^{1/3}\left(4k_1k_3 - k_2^2\right) - 2k_2\right] \tag{14}$$

$$\theta = \frac{1}{4}\left[\left(6k_1k_2k_3 - k_2^3 - 12k_3^2\epsilon\right) + \sqrt{\left(4k_1k_3 - k_2^2\right)^3 + \left(6k_1k_2k_3 - k_2^3 - 12k_3^2\epsilon\right)^2}\right] \tag{15}$$

$$\epsilon = -\frac{1}{12}\left(6u_0x^2 + 2u_1x^3 + u_2x^4 + 12C_1x + 12C_2\right) \tag{16}$$

$$u_0 = j(T_c - T_h)(S_1T_h + 2S_2T_h^2)/L - j^2\rho_1 \tag{17}$$

$$u_1 = j(T_c - T_h)(S_1 + 4S_2T_h)(T_c - T_h)/L(L - j^2\rho_2) \tag{18}$$

$$u_2 = j(T_c - T_h)2S_2(T_c - T_h)^2/L^2(L - j^2\rho_3) \tag{19}$$

$$C_1 = \frac{1}{L}\left[k_1(T_c - T_h) + \frac{1}{2}k_2\left(T_c^2 - T_h^2\right) + \frac{1}{3}k_3\left(T_c^3 - T_h^3\right) - \frac{1}{2}u_0L^2 - \frac{1}{6}u_1L^3 - \frac{1}{12}u_2L^4\right] \tag{20}$$

$$C_2 = k_1T_h + \frac{1}{2}k_2T_h^2 + \frac{1}{3}k_3T_h^3 \tag{21}$$

Equations (7)–(16) describe the proposed mathematical model utilized in this study. The model is established by incorporating the system's physical principles and adopting the linearity assumptions inherent to the model. Through the fitting process of the model to experimental data, the parameters specified in Section 2.1 were determined.

3. Experimental Data

As part of the experimental setup, a TEG1-12611-6.0 thermoelectric module manufactured by TECTEG MFR [36] is subjected to a current sweep under various temperature differences between the hot and cold sides of the module. The experimental setup comprises an oscilloscope, a multimeter, and thermocouples, which form the instrumentation component. Additionally, auxiliary control electronics are integrated to regulate the temperature of the heat source and heat sink, automate the measurement process, and maintain fixed and known temperature boundaries throughout the measurement process. The power output of a thermoelectric module can be represented as a function of the current, forming a parabolic curve that originates from the origin of the reference system (P vs. I). The curve is downward-opening and its vertex lies within the first quadrant, indicating the point of maximum power. This characteristic curve is obtained under fixed temperature difference conditions, and different temperature conditions at the cell boundaries yield distinct curves. The empirical relationship between power output and current, considering varying boundary temperature conditions, is illustrated by the curve depicted in Figure 2. The curve demonstrates a parabolic shape, commencing at the origin (0, 0), reaching a maximum at a specific current level. Beyond this point, any additional current generated by the cell leads to a decline in the electrical power output. These experimental findings serve as a crucial foundation for the study, forming the basis for the model fitting procedure.

To evaluate the power the TEG delivers, it is crucial to control the temperature of the hot side to ensure a consistent temperature gradient between the hot and cold sides. This is achieved using a heat source, an electric resistor that heats the hot side of the TEG. Conversely, the temperature of the cold side of the TEG is controlled through a heat exchanger system that employs water from a sizable reservoir at an ambient temperature of $T_{cold} = 24.3$ °C. The heat exchanger maintains a constant temperature on the cold side of the TEG, ensuring that the temperature boundaries remain fixed throughout the measurement process. This is important to ensure the accuracy and reproducibility of the results obtained from the TEG. To characterize the performance of the TEG, a controlled

load is used to drive a current sweep through the device. The current and output voltage are measured using an oscilloscope, which allows for accurate and precise measurements of the electrical properties of the TEG. By varying the load and measuring the resulting electrical characteristics of the TEG, it is possible to drown the P vs. I curve.

The experimental procedure involves subjecting the specimen to six distinct high-temperature conditions, namely $T_H = 60\,°C$, $70\,°C$, $80\,°C$, $90\,°C$, $100\,°C$, and $110\,°C$. The experimental tests were developed and explained in one of our previous works [25], with the following results presented in Figure 2.
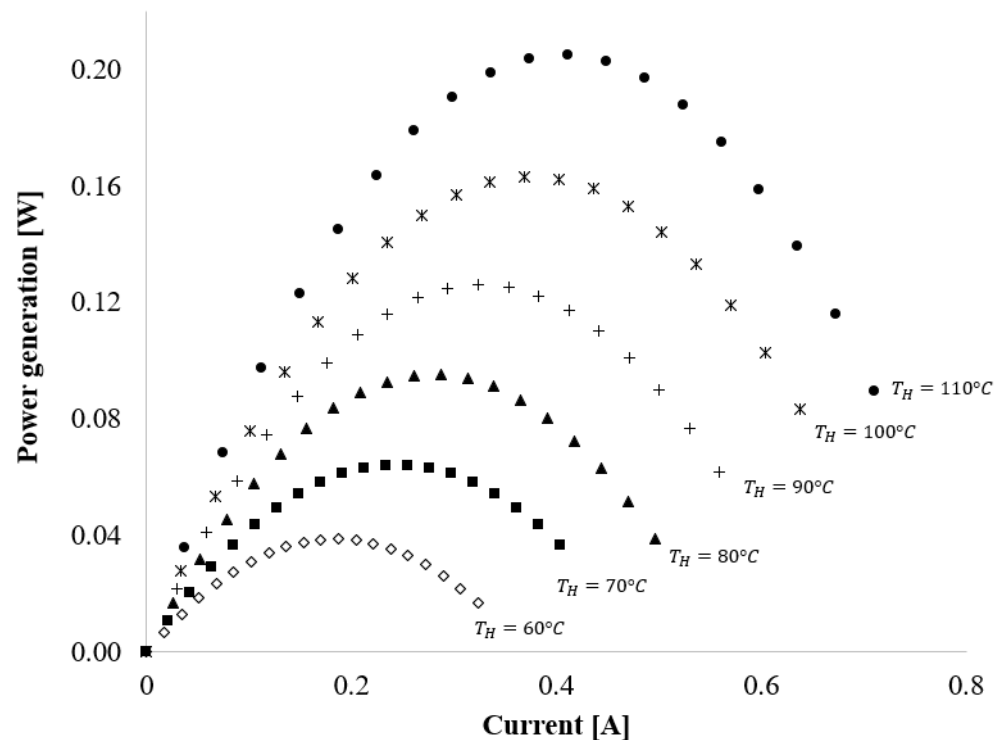

Figure 2. Variation of TEG Output Power (P_{output}) with Different Hot-Side Temperature Conditions at a Constant Cold-Side Temperature ($T_{cold} = 24.3\,°C$). Adapted from [25].

The mathematical model is subjected to a metaheuristic technique to identify the optimal parameter values that best fit the model's predictions and the experimental data across all temperature gradients presented in Figure 2.

4. Comparison Methods

To evaluate the efficacy of the proposed methodology, we employed two optimization algorithms, namely Particle Swarm Optimization (PSO) and Vortex Search Algorithm (VSA). The selection of PSO was based on its proven success in solving parameter estimation problems in electrical devices such as photovoltaic (PV) panels and motors, as reported in previous studies [37–39]. PSO is an iterative process that utilizes a swarm of particles to explore the solution space, guided by cognitive and social factors, leading to high-quality solutions. In this study, we fine-tuned PSO using the same methodology as the previously proposed SSA algorithm, resulting in optimized values for the following parameters: population size (50), the maximum number of iterations (1000), cognitive (0.0613) and social factors (1.5456), and initial (0.3246) and final inertias (0.9945). On the other hand, VSA mimics the behavior of fluid to explore the solution space by generating a vortex with a variable radius and center that decreases its size as the optimization process progresses. This algorithm was selected based on its effectiveness in solving the problem at hand, as reported in [25]. In this study, we employed the parameters reported by the authors in the original paper for the VSA.

5. Simulation Results

In this section, we present the outcomes obtained from assessing the master-stage methodologies within the designated test scenario, as described in Section 2. The evaluation of these methodologies focused on gauging their efficacy and resilience based on criteria such as minimum and average solutions, standard deviation, and average processing times. In order to accomplish this, we ran each methodology 1000 times using Matlab 2023 on a workstation with the Windows 11 Pro operating system. The workstation is equipped with an Intel(R) Xeon(R) E5-1660 v3 3.0 GHz processor, 16 GB DDR4 RAM, and a 2.5″ solid-state hard drive with 480 GB of storage. The findings, outlined in Table 2, present an overview of the optimization technique employed, along with the minimum and average values of the RMSE. Additionally, the table includes the standard deviation presented as a percentage and the average processing time measured in seconds.

In addition, the proposed optimization methodologies' optimized parameters, which accurately represent the thermoelectric generator, are presented in Table 3. These parameters serve as a reference for future studies and aid in comparing various optimization techniques. The discrepancies observed in the optimized solutions emphasize the problem's complexity due to the numerous variables and non-linearities involved, resulting in a vast solution space.

Table 2. Results obtained by the master–slave optimization methodologies proposed.

Method	Minimum RMS Error	Average RMS Error	Standard Deviation (%)	Processing Time (s)
SSA	0.0018	0.0021	6.8444	209.9596
PSO	0.0017	0.0019	10.3785	225.8748
VSA	0.0018	0.0021	8.4311	212.1074

Table 3. Parameters acquired through the optimal solution for each method (Minimum RSME).

Method	k_1	k_2	k_3	S_0	S_1	S_2	ρ_0	ρ_1	ρ_2	n_{legs}	A_{cs}
SSA	6.3014	-3.00×10^{-2}	4.26×10^{-5}	1.84×10^{-5}	8.39×10^{-7}	-1.09×10^{-9}	4.80×10^{-7}	1.57×10^{-8}	6.81×10^{-11}	66.00	1.004×10^{-6}
PSO	6.2854	-3.05×10^{-2}	4.54×10^{-5}	2.44×10^{-5}	8.38×10^{-7}	-1.09×10^{-9}	4.60×10^{-7}	1.470×10^{-8}	6.91×10^{-11}	64.00	9.89×10^{-7}
VSA	6.0609	-3.05×10^{-2}	4.36×10^{-5}	1.62×10^{-5}	8.38×10^{-7}	-1.09×10^{-9}	5.25×10^{-7}	1.50×10^{-8}	6.79×10^{-11}	67.00	1.004×10^{-6}

First, it can be observed that all three methods perform similarly, with average RMSE errors ranging from 0.0019 W to 0.0021 W, indicating that each method can achieve an accurate estimation of the parameters. Additionally, the minimum RMSE errors for each method are relatively low, ranging from 0.0017 W to 0.0018 W, suggesting that the methods effectively find a good solution to the MINLP problem. However, when considering the standard deviation of the RMSE errors, PSO has a higher value of 10.3785%, while SSA and VSA have lower values of 6.8444% and 8.4311%, respectively. This indicates that the solutions obtained by PSO are more dispersed than those obtained by SSA and VSA and that the latter two methods are more consistent in producing similar results across multiple runs. Furthermore, when examining the processing time, it can be seen that there is not a significant difference between the methods, with processing times ranging from 209.9596 to 225.8748 s. This suggests that all methods are computationally efficient and can be used for other large-scale optimization problems. Overall, the results of this analysis indicate that the three metaheuristic optimization techniques effectively solve the parameter estimation problem for TEG module, with similar average RMSE errors and processing times. However, there are differences in the consistency of the solutions obtained, with PSO having a higher standard deviation of the RMSE errors compared to SSA and VSA. Therefore, based on this analysis, SSA and VSA may be preferred over PSO for this particular problem due to their ability to produce more consistent results.

Figure 3 illustrates each method's error evolution for a single random run. The figure exhibits that all the methods exhibit a prompt convergence towards the minimum error.

Nonetheless, the PSO algorithm demonstrates superior performance over the SSA and VSA algorithms regarding convergence speed, achieving the minimum error in considerably fewer iterations. The error reduction occurs in each iteration per the optimization algorithm method expounded in Section 2. The PSO algorithm employs an evolutionary strategy that iteratively updates the velocity and position of each particle based on the best solution attained by the particle and its neighboring particles. This approach facilitates a rapid convergence to the optimal solution, requiring fewer iterations than alternative methods.
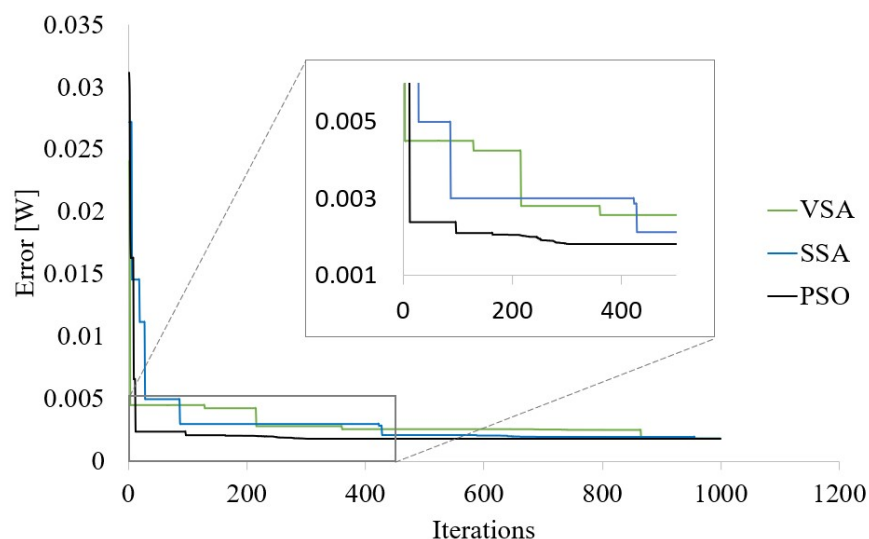
Figure 3. Evolution of the error of each method towards the optimal parameter estimation solution.

By evaluating the relationship between the performance parameters of each method, it is possible to find the method for this specific problem.

Upon analyzing the results presented in Figures 4 and 5, it is evident that the method with the shortest line connecting to the origin provides better performance in terms of standard deviation and time compared to the average RMSE. Specifically, the SSA exhibits superior performance, followed by the VSA and PSO. Notably, a consistent relationship between average time and RMSE is observed across these methods. Although the differences in execution time between methods are small (less than 4 s), they become significant when considering the aging of TEG modules and their evolving thermophysical properties. Therefore, it is necessary to periodically conduct this study for each TEG module in a complete system. As the number of modules to be tested increases, even a few seconds of saved time can translate into significant time savings in industrial applications.

The RMSE values of the SSA and VSA were found to be in close proximity, differing only by 0.5×10^{-3}. However, a significant difference in their standard deviations was observed in Figure 6. Based on the results obtained in this study, it was found that the standard deviation of the SSA was 34.0% lower than that of the VSA and 18.8% lower than that of the PSO. Therefore, it can be inferred that the SSA is the most effective method among the three algorithms for this particular problem. It should be noted that the numerical magnitudes of the standard deviations follow the order of $SSA < VSA < PSO$.

In our previous work [25], we discussed three heuristic methods to estimate the operation parameters of a TEG, namely the VSA, CGA, and CSA. In this paper, we have developed two new algorithms to optimize the response compared to our previous results. We have also included a different approach to analyzing the efficiency of these methods, including Figures 3–6. Our current work presents a better algorithm (SSA) to find the parameters with faster and more accurate results compared to our previous work.
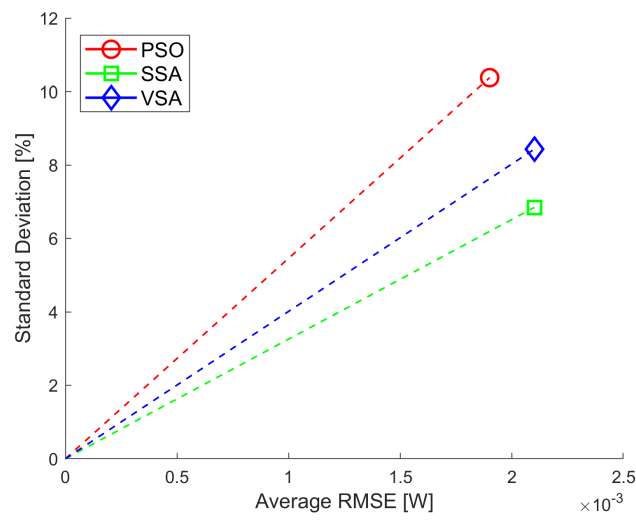
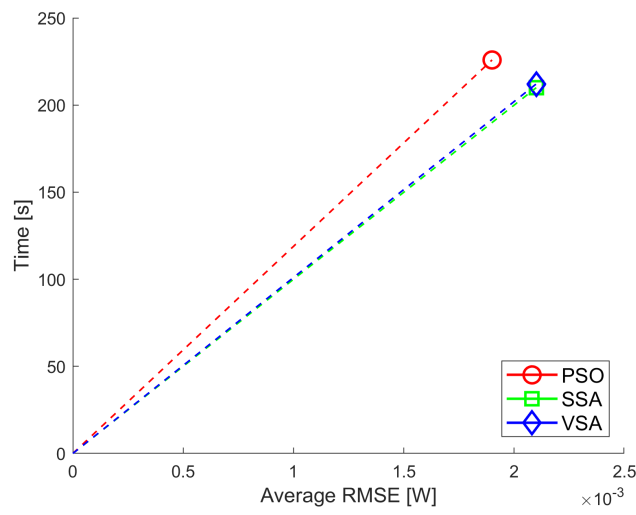**Figure 4.** Standard deviation vs. Average RMSE for each metaheuristic technique.

Figure 5. Time vs. Average RMSE for each metaheuristic technique.
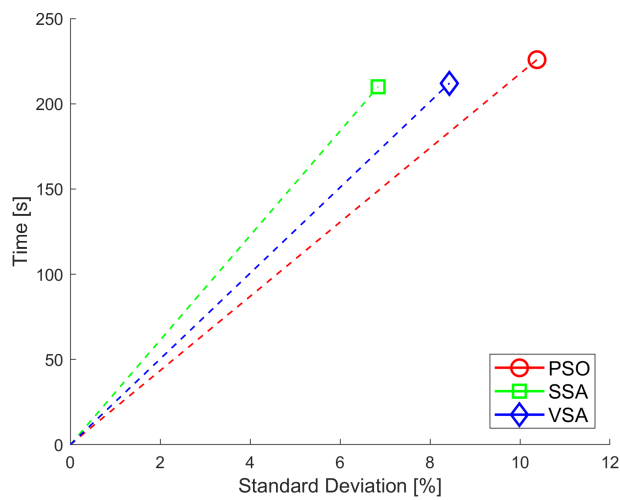

Figure 6. Relationship between standard deviation and time for each technique.

6. Conclusions

We presented an evaluation of three master–slave optimization methodologies for solving the MINLP problem of parameter estimation in thermoelectric generators. Our work contributes to the field by providing a comparison of optimization algorithms to solve the MINLP problem and evaluating their performance parameters, including average RMSE, the standard deviation of RMSE, and processing time.

The results showed that all three methods performed similarly in terms of average RMSE errors, but SSA and VSA had lower standard deviations, indicating their superior results, with a range of 0.0019 W to 0.0021 W, indicating that each method can accurately estimate the parameters. Furthermore, the minimum RMSE errors for each method were relatively low, ranging from 0.0017 W to 0.0018 W. Additionally, the average processing times for each method were relatively high, ranging from 209.9596 s to 225.8748 s, suggesting that they may not be practical for real-time applications. Our contribution is in providing valuable insights into the optimization of TEG modules in various practical applications. Furthermore, our findings indicate that the optimization method with the shortest line connecting to the origin demonstrates better performance in terms of standard deviation and processing time compared to the average RMSE. We conclude that SSA outperformed the VSA and PSO methods in terms of overall performance.

However, we acknowledge that our study has some limitations, including the use of a single test scenario and the assumption of a linear relationship between temperature conditions and thermoelectric properties. Future studies could address these limitations by testing the methods in more complex scenarios and by considering nonlinear relationships between temperature and thermoelectric properties. This work highlights the importance of effective optimization techniques for accurate and rapid parameter estimation of thermoelectric generators. It provides a valuable comparison of optimization algorithms for time-saving and practical applications in the field. Our contribution will guide future studies to improve upon the limitations of this study and explore further ways to optimize TEG modules in various practical applications.

The optimized parameters derived from each method underscore the intricate nature of the problem, which is attributed to the multitude of variables and non-linearities involved. This complexity contributes to the expansive solution space. These parameters serve as a valuable reference for future research and enable effective comparison among various optimization approaches. Overall, this study contributes to the advancement of optimization techniques for parameter estimation in thermoelectric generators, and future research could focus on developing hybrid optimization methods that combine the strengths of different approaches to improve the robustness and efficiency of the parameter estimation process.

Author Contributions: Conceptualization, methodology, software, and writing (review and editing), D.S.-V., O.D.M., W.G.-G., L.F.G.-N. and A.-J.P.-M. All authors read and agreed to the published version of the manuscript.

Conflicts of Interest: The authors of this paper declare no conflict of interest.

References

1. Bürger, A.; Zeile, C.; Altmann-Dieses, A.; Sager, S.; Diehl, M. A Gauss-Newton-Based Decomposition Algorithm for Nonlinear Mixed-Integer Optimal Control Problems. 2022. Available online: https://www.sciencedirect.com/science/article/pii/S000510982300119X (accessed on 10 March 2022).
2. Harjunkoski, I.; Westerlund, T.; Pörn, R. Numerical and environmental considerations on a complex industrial mixed integer non-linear programming (MINLP) problem. *Comput. Chem. Eng.* **1999**, *23*, 1545–1561. [CrossRef]

3.   Epelle, E.I.; Gerogiorgis, D.I. Mixed-Integer Nonlinear Programming (MINLP) for production optimisation of naturally flowing and artificial lift wells with routing constraints. *Chem. Eng. Res. Des.* **2019**, *152*, 134–148. [CrossRef]

4.   Boukouvala, F.; Misener, R.; Floudas, C.A. Global optimization advances in mixed-integer nonlinear programming, MINLP, and constrained derivative-free optimization, CDFO. *Eur. J. Oper. Res.* **2016**, *252*, 701–727. [CrossRef]

5.   Yiqing, L.; Xigang, Y.; Yongjian, L. An improved PSO algorithm for solving non-convex NLP/MINLP problems with equality constraints. *Comput. Chem. Eng.* **2007**, *31*, 153–162. [CrossRef]

6.   Santos, L.F.; Costa, C.B.; Caballero, J.A.; Ravagnani, M.A. MINLP model for work and heat exchange networks synthesis considering unclassified streams. In *Computer Aided Chemical Engineering*; Elsevier: Amsterdam, The Netherlands, 2022; Volume 51, pp. 793–798.

7.   Yue, D.; You, F. Sustainable scheduling of batch processes under economic and environmental criteria with MINLP models and algorithms. *Comput. Chem. Eng.* **2013**, *54*, 44–59. [CrossRef]

8.   Schlueter, M.; Erb, S.O.; Gerdts, M.; Kemble, S.; Rückmann, J.J. MIDACO on MINLP space applications. *Adv. Space Res.* **2013**, *51*, 1116–1131. [CrossRef]

9.   Su, L.; Tang, L.; Grossmann, I.E. Computational strategies for improved MINLP algorithms. *Comput. Chem. Eng.* **2015**, *75*, 40–48. [CrossRef]

10.   Kronqvist, J.; Lundell, A. Convex Minlp–An Efficient Tool for Design and Optimization Tasks? In *Computer Aided Chemical Engineering*; Elsevier: Amsterdam, The Netherlands, 2019; Volume 47, pp. 245–250.

11.   Li, C.; Han, P.; Zhou, M.; Gu, M. Design of multimodal hub-and-spoke transportation network for emergency relief under COVID-19 pandemic: A meta-heuristic approach. *Appl. Soft Comput.* **2023**, *133*, 109925. [CrossRef]

12.   Leo, E.; Engell, S. Condition-based maintenance optimization via stochastic programming with endogenous uncertainty. *Comput. Chem. Eng.* **2022**, *156*, 107550. [CrossRef]

13.   Thang, V.; Ha, T.; Li, Q.; Zhang, Y. Stochastic optimization in multi-energy hub system operation considering solar energy resource and demand response. *Int. J. Electr. Power Energy Syst.* **2022**, *141*, 108132. [CrossRef]

14.   Wang, Y.C.; Chen, T. A Bi-objective AHP-MINLP-GA approach for Flexible Alternative Supplier Selection amid the COVID-19 pandemic. *Soft Comput. Lett.* **2021**, *3*, 100016. [CrossRef]

15.   Chen, D.; Luo, Y.; Yuan, X. Cascade refrigeration system synthesis based on hybrid simulated annealing and particle swarm optimization algorithm. *Chin. J. Chem. Eng.* **2022**, *in press.* [CrossRef]

16.   Mohammed, A.M.; Duffuaa, S.O. A tabu search based algorithm for the optimal design of multi-objective multi-product supply chain networks. *Expert Syst. Appl.* **2020**, *140*, 112808. [CrossRef]

17.   Nimmanterdwong, P.; Chalermsinsuwan, B.; Piumsomboon, P. Optimizing utilization pathways for biomass to chemicals and energy by integrating emergy analysis and particle swarm optimization (PSO). *Renew. Energy* **2023**, *202*, 1448–1459. [CrossRef]

18.   Yavuz, A.; Celik, N.; Chen, C.H.; Xu, J. A Sequential Sampling-based Particle Swarm Optimization to Control Droop Coefficients of Distributed Generation Units in Microgrid Clusters. *Electr. Power Syst. Res.* **2023**, *216*, 109074. [CrossRef]

19.   Tubishat, M.; Idris, N.; Shuib, L.; Abushariah, M.A.; Mirjalili, S. Improved Salp Swarm Algorithm based on opposition based learning and novel local search algorithm for feature selection. *Expert Syst. Appl.* **2020**, *145*, 113122. [CrossRef]

20.   Çelik, E.; Öztürk, N.; Arya, Y. Advancement of the search process of salp swarm algorithm for global optimization problems. *Expert Syst. Appl.* **2021**, *182*, 115292. [CrossRef]

21.   Dahou, A.; Abd Elaziz, M.; Chelloug, S.A.; Awadallah, M.A.; Al-Betar, M.A.; Al-qaness, M.A.; Forestiero, A. Intrusion Detection System for IoT Based on Deep Learning and Modified Reptile Search Algorithm. *Comput. Intell. Neurosci.* **2022**, *2022*, 6473507. [CrossRef]

22.   Forestiero, A. Heuristic recommendation technique in Internet of Things featuring swarm intelligence approach. *Expert Syst. Appl.* **2022**, *187*, 115904. [CrossRef]

23.   Sanin-Villa, D. Recent Developments in Thermoelectric Generation: A Review. *Sustainability* **2022**, *14*, 16821. [CrossRef]

24.   Sanin-Villa, D.; Monsalve-Cifuentes, O.D.; Henao-Bravo, E.E. Evaluation of Thermoelectric Generators under Mismatching Conditions. *Energies* **2021**, *14*, 8016. [CrossRef]

25.   Sanin-Villa, D.; Montoya, O.D.; Grisales-Noreña, L.F. Material Property Characterization and Parameter Estimation of Thermoelectric Generator by Using a Master–Slave Strategy Based on Metaheuristics Techniques. *Mathematics* **2023**, *11*, 1326. [CrossRef]

26.   Dong, C.; Shi, Y.; Li, Q.; Gu, H.; Li, D.; Ye, Y.; Li, T. An analysis on comprehensive influences of thermoelectric power generation based on waste heat recovery. *Case Stud. Therm. Eng.* **2023**, *44*, 102867. [CrossRef]

27.   Sanin-Villa, D.; Monsalve-Cifuentes, O.D.; Del Rio, J.S. Early fever detection on COVID-19 infection using thermoelectric module generators. *Int. J. Electr. Comput. Eng* **2021**, *11*, 3828–3837. [CrossRef]

28.   Tailin, L.; Youhong, L.; Yingzeng, Z.; Haodong, C.; Qingpei, X.; Jun, Z.; Rende, Z.; Yi, L.; Yongchun, X. Comprehensive modeling and characterization of Chang'E-4 radioisotope thermoelectric generator for lunar mission. *Appl. Energy* **2023**, *336*, 120865. [CrossRef]

29.   Sanin-Villa, D.; Henao-Bravo, E.; Ramos-Paja, C.; Chejne, F. Evaluation of Power Harvesting on DC-DC Converters to Extract the Maximum Power Output from TEGs Arrays under Mismatching Conditions. *J. Oper. Autom. Power Eng.* **2023**. [CrossRef]

30. Faris, H.; Mirjalili, S.; Aljarah, I.; Mafarja, M.; Heidari, A.A. Salp swarm algorithm: Theory, literature review, and application in extreme learning machines. In *Nature-Inspired Optimizers: Theories, Literature Reviews and Applications*; Springer: Cham, Swithzarland, 2020; pp. 185–199.

31. Sultan, H.M.; Menesy, A.S.; Kamel, S.; Selim, A.; Jurado, F. Parameter identification of proton exchange membrane fuel cells using an improved salp swarm algorithm. *Energy Convers. Manag.* **2020**, *224*, 113341. [CrossRef]

32. Rosales-Muñoz, A.A.; Montano, J.; Grisales-Noreña, L.F.; Montoya, O.D.; Andrade, F. Optimal Power Dispatch of DGs in Radial and Mesh AC Grids: A Hybrid Solution Methodology between the Salps Swarm Algorithm and Successive Approximation Power Flow Method. *Sustainability* **2022**, *14*, 13408. [CrossRef]

33. Abualigah, L.; Shehab, M.; Alshinwan, M.; Alabool, H. Salp swarm algorithm: A comprehensive survey. *Neural Comput. Appl.* **2020**, *32*, 11195–11215. [CrossRef]

34. Wee, D. Analysis of thermoelectric energy conversion efficiency with linear and nonlinear temperature dependence in material properties. *Energy Convers. Manag.* **2011**, *52*, 3383–3390. [CrossRef]

35. Ju, C.; Dui, G.; Zheng, H.H.; Xin, L. Revisiting the temperature dependence in material properties and performance of thermoelectric materials. *Energy* **2017**, *124*, 249–257. [CrossRef]

36. TECTEG MFR. Div. of Thermal Electronics Corp. Specifications TEG Module TEG1-12611-6.0. 2022. Available online: https://tecteg.com/wp-content/uploads/2014/09/SpecTEG1-12611-6.0TEG-POWERGENERATOR-new.pdf (accessed on 9 January 2022).

37. Kumari, P.A.; Geethanjali, P. Parameter estimation for photovoltaic system under normal and partial shading conditions: A survey. *Renew. Sustain. Energy Rev.* **2018**, *84*, 1–11. [CrossRef]

38. Liu, Z.H.; Wei, H.L.; Li, X.H.; Liu, K.; Zhong, Q.C. Global identification of electrical and mechanical parameters in PMSM drive based on dynamic self-learning PSO. *IEEE Trans. Power Electron.* **2018**, *33*, 10858–10871. [CrossRef]

39. Jordehi, A.R. Enhanced leader particle swarm optimisation (ELPSO): An efficient algorithm for parameter estimation of photo-voltaic (PV) cells and modules. *Sol. Energy* **2018**, *159*, 78–87. [CrossRef]